Neuron, Vol. 36, 31–43, September 26, 2002, Copyright ©2002 by Cell Press

Changing Requirements for *Gbx2* in Development of the Cerebellum and Maintenance of the Mid/Hindbrain Organizer

James Y.H. Li,[1,2] Zhimin Lao,[1] and Alexandra L. Joyner[1,2,3,4]
[1]Howard Hughes Medical Institute and Developmental Genetics Program
Skirball Institute of Biomolecular Medicine
[2]Department of Cell Biology
[3]Department of Physiology and Neuroscience
New York University School of Medicine
540 First Avenue
New York, New York 10016

Summary

We examined whether *Gbx2* is required after embryonic day 9 (E9) to repress *Otx2* in the cerebellar anlage and position the midbrain/hindbrain organizer. In contrast to *Gbx2* null mutants, mice lacking *Gbx2* in rhombomere 1 (r1) after E9 (*Gbx2*-CKO) are viable and develop a cerebellum. A *Gbx2*-independent pathway can repress *Otx2* in r1 after E9. Mid/hindbrain organizer gene expression, however, continues to be dependent on *Gbx2*. We found that *Fgf8* expression normally correlates with the isthmus where cells undergo low proliferation and that in *Gbx2*-CKO mutants this domain is expanded. We propose that *Fgf8* permits lateral cerebellar development through repression of *Otx2* and also suppresses medial cerebellar growth in *Gbx2*-CKO embryos. Our work has uncovered distinct requirements for *Gbx2* during cerebellum formation and provided a model for how a transcription factor can play multiple roles during development.

Introduction

Regionalization of the central nervous system (CNS) is a complex developmental process that involves integration of both cell extrinsic and intrinsic events. Development of the cerebellum is an ideal model system for studying how coordination of such events leads to patterning within the CNS. The cerebellum is one of the simplest CNS structures, as it is composed of only a few cell types arranged in three distinct layers. In addition, the primary events of cerebellar development are well characterized. The cerebellum is derived from the dorsal portion (alar plate) of rhombomere 1 (r1), which lies immediately posterior to the mesencephalon (mes), the embryonic primordium of the midbrain (Wingate, 2001). The posterior edges of the alar plate of r1, called the anterior rhombic lips, give rise to cerebellar granule cells, whereas the ventricular layer of the more anterior alar plate produces all other cerebellar cell types (Hatten and Heintz, 1995).

A number of extrinsic and intrinsic proteins expressed in the mes and r1 (mes/r1) region have been identified, and their functional requirements in cerebellar development have been demonstrated in the past decade (Joyner et al., 2000; Liu and Joyner, 2001). Among these factors, Wnt1 and Fgf8 are two secreted factors that are expressed at the mes/r1 junction and are essential for the activity of a local signaling center, the mid/hindbrain organizer, which regulates formation of the midbrain and cerebellum. When placed in a competent brain region, Fgf8-soaked beads can mimic the mes/r1 junction and induce midbrain or cerebellar gene expression and in some cases development of ectopic structures (Crossley et al., 1996; Garda et al., 2001; Liu et al., 1999; Martinez et al., 1999; Shamim et al., 1999).

The details of the cell intrinsic events that govern the differential development of the midbrain versus the cerebellum in response to *Fgf8* remain to be elucidated. However, a number of studies have indicated that *Otx2* and *Gbx2*, two homeobox genes that are expressed in the mes and r1, respectively, are critical intrinsic factors required for specification of the midbrain versus cerebellum, since the midbrain or r1-3 fail to develop in mouse embryos lacking *Otx2* or *Gbx2*, respectively (Acampora et al., 1995; Ang et al., 1996; Matsuo et al., 1995; Wassarman et al., 1997). *Otx2* and *Gbx2* divide the neuroectoderm into anterior and posterior domains with a common border at the presumptive mid/hindbrain junction by E7.5 (Ang et al., 1994; Bouillet et al., 1995; Wassarman et al., 1997). *Wnt1*, *Fgf8*, and other mes/r1 genes then become activated near the *Otx2*/*Gbx2* border around E8.5. After E9.5, *Gbx2* expression is maintained in the alar plate of r1, and the expression of *Wnt1* and *Fgf8* becomes restricted to adjacent narrow domains with a sharp common border that coincides with the *Otx2*/*Gbx2* border. Furthermore, experiments in chick and mouse have shown that the Fgf8b isoform can repress *Otx2* expression and induce *Gbx2* (Garda et al., 2001; Liu et al., 1999; Martinez et al., 1999; Sato et al., 2001; Shamim et al., 1999) and in some cases can transform the mes into a cerebellum (Martinez et al., 1999; Sato et al., 2001). These results raise the question of whether *Gbx2* is a cell intrinsic factor that mediates *Fgf8* induction of a cerebellum.

It has not been possible to determine the specific role of *Gbx2* in cerebellar development from *Fgf8* misexpression experiments or analysis of *Gbx2* null mutants, since in these studies expression of many genes, including *Otx2* and *Gbx2*, is altered simultaneously. For example, *Otx2* expression rapidly expands posteriorly into r1-3 in *Gbx2* null mutants by the late headfold stage (E7.75), correlating with a transformation of this region into a mesencephalic fate (Li and Joyner, 2001; Martinez-Barbera et al., 2001; Millet et al., 1999). One interpretation of this result is that repression of *Otx2* by *Gbx2* at E7.75 is essential for normal development of r1-3. Indeed, we showed that removal of *Otx2* in *Gbx2* null mutant embryos rescues development of r3, demonstrating that repression of *Otx2* by *Gbx2* is essential for normal development in r3 (Li and Joyner, 2001). Furthermore, in *Otx2*/*Gbx2* double mutants the mes/r1 region expresses both midbrain and r1 genes (*Wnt1*, *Fgf8*, and others) (Li and Joyner, 2001; Martinez-Barbera et al., 2001), demonstrating essential roles of *Otx2* and *Gbx2* in defining the

[4]Correspondence: joyner@saturn.med.nyu.edu

complementary *Wnt1* and *Fgf8* expression domains and thus normal function of the mid/hindbrain organizer. Since mouse embryos deficient for both *Otx2* and *Gbx2* fail to develop a morphologically distinct cerebellum, it is not clear whether *Gbx2* is required to induce cerebellum development or to repress additional midbrain genes like *Wnt1*. In addition, it remains to be tested whether sustained expression of *Gbx2* in r1 continues to play a role in maintaining a functional mid/hindbrain organizer.

To investigate the sequential roles of *Gbx2* in cerebellar development and maintenance of the mid/hindbrain organizer, we generated a conditional mouse mutant of *Gbx2* using the *Cre/loxP* system and removed *Gbx2* function in r1 between the 8 somite stage (E8.5) and the 15 somite stage (E9). Our studies uncovered a *Gbx2*-independent pathway to repress *Otx2* after E9 and that embryos deficient in *Gbx2* after E9 in r1 form a cerebellum, with variable defects only in the medial region (the vermis). Furthermore, *Gbx2* continues to play a critical role in positioning and maintaining normal mid/hindbrain organizer function after E9.

Results

Generation of *Gbx2* Conditional Mutant Mice

To study the sequential roles of *Gbx2* in cerebellar development and maintenance of the mid/hindbrain organizer after E8.5, we generated mice carrying a conditional *Gbx2* mutant allele, $Gbx2^{flox}$ (Figures 1A–1C). No abnormal phenotypes were detected in $Gbx2^{flox/flox}$ or $Gbx2^{-/flox}$ mice ($Gbx2^{-}$ designates the original *Gbx2* null allele; Wassarman et al., 1997), demonstrating that the $Gbx2^{flox}$ allele has wild-type activity. To test whether Cre-mediated conversion of the $Gbx2^{flox}$ allele into a deletion allele ($Gbx2^{\Delta hd}$) disrupts *Gbx2* function, we crossed $Gbx2^{+/flox}$ mice with *CMV-Cre* transgenic mice that express *Cre* broadly. $Gbx2^{+/\Delta hd}$ mice were identified and bred with $Gbx2^{+/-}$ mice. Similar to our previously described $Gbx2^{-/-}$ mice (Wassarman et al., 1997), no $Gbx2^{-/\Delta hd}$ mice were recovered at weaning. In addition, $Gbx2^{-/\Delta hd}$ embryos at E18.5 displayed the same phenotypes as $Gbx2^{-/-}$ embryos (data not shown). Therefore, Cre-mediated excision converts the wild-type $Gbx2^{flox}$ allele into a null $Gbx2^{\Delta hd}$ allele.

Specific Deletion of *Gbx2* in r1 after E8.5

To remove *Gbx2* specifically in r1 after E8.5, we used the $En1^{+/Cre}$ mouse line in which *Cre* was inserted into the first exon of *En1* by gene targeting (Kimmel et al., 2000). We analyzed Cre activity in the neural tube in detail by crossing $En1^{+/Cre}$ mice with *R26R lacZ* reporter mice in which cells express β-gal activity after Cre-mediated recombination (Soriano, 1999). In X-gal-stained double transgenic embryos, Cre activity was initially detected in the presumptive mes/r1 junction area at the 5 somite stage (data not shown). By the 8 somite stage, β-gal activity was detected broadly in the mes and anterior r1 (Figure 1D). At E9.5, virtually all cells in the midbrain and r1 produced β-gal activity, as revealed by X-gal staining of whole-mount embryos and sections, indicating that Cre-mediated recombination occurs in all midbrain and r1 cells by E9.5 (Figures 1E and 1F).

We then crossed $Gbx2^{flox/flox}$ mice with double heterozygous $En1^{Cre}$ $Gbx2^{-}/En1^{+}$ $Gbx2^{+}$ mice. As mouse *En1* and *Gbx2* are closely linked (Chapman et al., 1997), approximately 50% of the progeny from such crosses had the genotype $En1^{Cre}$ $Gbx2^{-}/En1^{+}$ $Gbx2^{flox}$, referred to as *Gbx2*-CKO (for Conditional Knocked-Out), and the other 50% of the progeny were $En1^{+}$ $Gbx2^{+}/En1^{+}$ $Gbx2^{flox}$ and used as wild-type controls. In *Gbx2*-CKO embryos, Cre-mediated conversion should produce a $Gbx2^{-/\Delta hd}$ genotype in *En1*-expressing cells. We analyzed *Gbx2* expression in *Gbx2*-CKO embryos to confirm the loss of *Gbx2* in r1. At the 6 somite stage, *Gbx2* expression appeared normal in *Gbx2*-CKO embryos (data not shown). By the 8 somite stage, however, the anterior-most *Gbx2* expression in r1, which overlaps with the *En1* expression domain, was absent (Figure 2B and see Figure 1D). In wild-type embryos, the initial *Gbx2* expression in r1-3 at E8.5 becomes restricted to a transverse ring at the mes/r1 junction and the alar plate of r1 by E9.5 (Figures 2C and 2E). By E9 (15 somites) when *En1* expression has expanded throughout r1 (see Figures 1E and 1F), *Gbx2* expression was completely absent from r1 but was normal in the spinal cord of *Gbx2*-CKO embryos (Figures 2D and 2F). Therefore, in *Gbx2*-CKO embryos, *Gbx2* is expressed normally until the 6 somite stage, and thereafter *Gbx2* is progressively lost from anterior to posterior in r1 such that by E9 *Gbx2* expression in r1 is completely abolished.

The Cerebellum Forms in *Gbx2*-CKO Mice

When $Gbx2^{flox/flox}$ mice were crossed with $En1^{Cre}$ $Gbx2^{-}/En1^{+}$ $Gbx2^{+}$ mice, a normal frequency of *Gbx2*-CKO mice were recovered at E18.5 (n = 13/30), 1 day prior to parturition. After birth, some *Gbx2*-CKO pups were found dead before weaning. However, in contrast to the 100% penetrant neonatal lethality of *Gbx2* null mutants, more than half of *Gbx2*-CKO mutants survived past weaning (Figure 3A). The surviving mutants were smaller than their littermates, with a lower body weight, but both males and females were viable and fertile and nursed their pups normally (Figures 3B and 3C).

Interestingly, *Gbx2*-CKO mice showed no apparent defects in motor coordination, suggesting these mutant mice had a functional cerebellum. Indeed, examination of the brains of adult *Gbx2*-CKO mice revealed that the cerebellum developed in these mice. In normal adult mice, the cerebellum is divided into a middle region called the vermis and two lateral extensions called the hemispheres (Figure 3D), and each region has a characteristic foliation pattern (Figures 3E and 3F). In *Gbx2*-CKO mice, the cerebellar hemispheres were remarkably normal (Figures 3G, 3I, 3J, and 3L), whereas the vermis was smaller than normal, and the foliation pattern was disrupted (Figures 3G, 3H, 3J, and 3K). In addition, the lateral regions of the posterior midbrain (inferior colliculi) appeared slightly enlarged (Figures 3G and 3J). There were variations in the vermis phenotype among *Gbx2*-CKO mice. In more severely affected mice (n = 4/6), the vermis was greatly reduced, with the lateral hemispheres appearing to extend and meet at the midline (Figure 3G). In *Gbx2*-CKO mutants with a less severe phenotype (n = 2/6), the vermis was more discernable, but the folia were reduced in size (Figure 3J). Analysis of serial sections of *Gbx2*-CKO cerebella showed that,

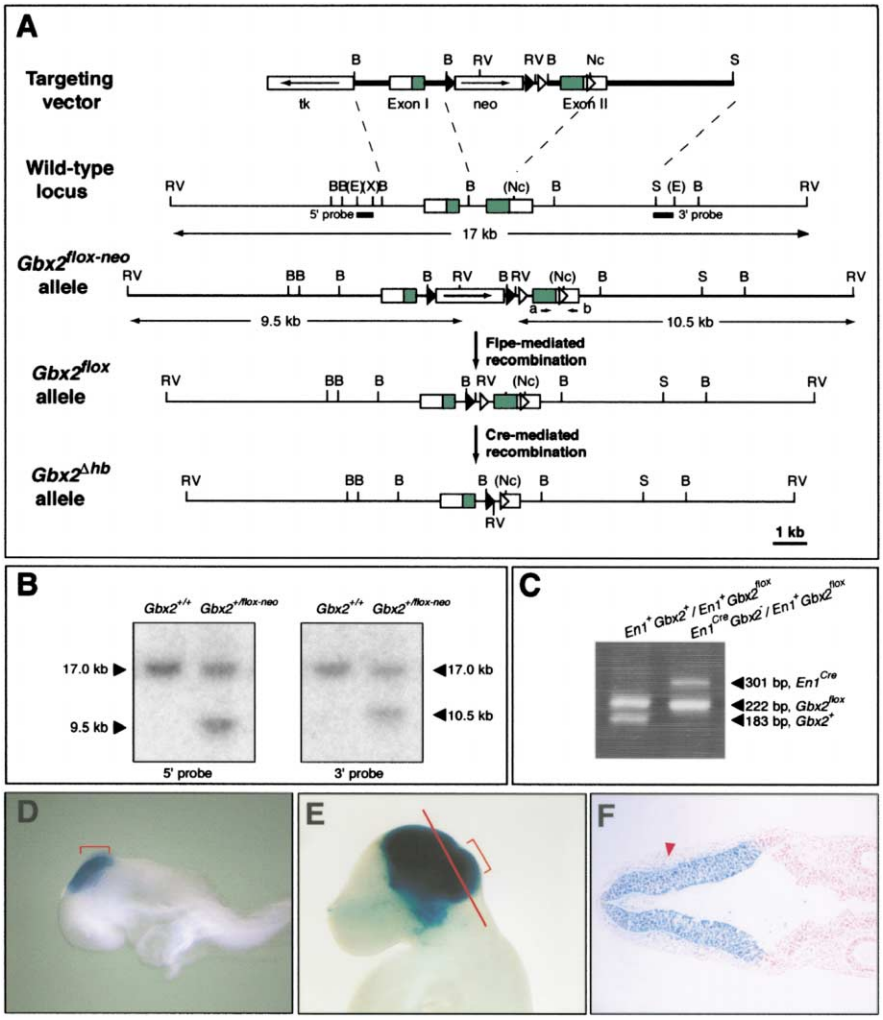

Figure 1. Generation of a *Gbx2* Conditional *loxP* Mutant Allele and Detection of Cre Activity in *En1*$^{+/Cre}$ Mice

(A) Schematic representation of gene targeting strategy. The thicker lines in the targeting construct represent *Gbx2* genomic DNA, with an insertion of one *loxP* site (empty triangle) in the NocI site and another in the BamHI site along with a *neo* cassette flanked with *frt* sites (filled triangles). The 3 kb BamHI-BamHI and 5 kb NcoI-SalI *Gbx2* genomic fragments were used for homologous recombination. Boxes represent the two *Gbx2* exons (exon I and II) and the *neo* and *tk* cassettes. The protein coding regions are indicated by green, and the orientation of transcription of the *neo* and *tk* cassettes is indicated by arrows within the boxes. Relevant restriction enzyme sites indicated are B, BamHI; E, EcoRI; Nc, NcoI; Rv, EcoRV; X, XbaI; S, SalI. The restriction enzyme sites in parentheses are shown only for selected sites. PCR primers a and b used for genotyping are shown as small arrows, and the 5′ (520 bp, EcoRI/XbaI) and 3′ (750 bp, SalI/EcoRI) external probes for Southern blot analysis are indicated as lines.

(B) Southern blot analysis of *Gbx2*$^{+/flox\text{-}neo}$ ES cell clones. Following EcoRV digestion of DNA, the 5′ and 3′ probes identify the wild-type allele as a 17.0 kb fragment and the mutant allele as 9.5 and 10.5 kb fragments, respectively.

(C) Genotyping *En1*^{Cre} *Gbx2*$^{-}$/*En1*$^{+}$ *Gbx2*^{flox} and *En1*$^{+}$ *Gbx2*$^{+}$/*En1*$^{+}$ *Gbx2*^{flox} mice by PCR. The *En1*^{Cre}, *Gbx2*^{flox}, and *Gbx2*$^{+}$ alleles produce PCR products of 301, 222, and 183 bp, respectively.

(D–F) Expression of Cre activity revealed by X-gal staining of *En1*$^{+/Cre}$; *R26R lacZ*$^{+/-}$ embryos at the 8 somite stage (D) and E9.5 (E and F). (F) A coronal section of the embryo in (E), showing that Cre-mediated DNA recombination has occurred in essentially all cells in the midbrain and r1. The plane of sectioning is shown in (F) as a red line. Brackets indicate expression of Cre activity initially in the anterior portion of r1 (D) and then in all of r1 (E).

except for the most posterior lobule X, all lobules were reduced in size to varying degrees, with lobules V and IX being less affected (Figures 3H and 3K). Interestingly, lobules V, IX, and X are the first three lobules to form (Millen et al., 1994). In spite of the morphological defects, the cerebellar cytoarchitecture in *Gbx2*-CKO mutants appeared normal (Figures 3 and 4 and data not shown). In summary, deletion of *Gbx2* in r1 by E9 results in repressed development of the cerebellar vermis, whereas development of the cerebellar hemispheres and the cytoarchitecture of the cerebellum are essentially normal.

Development of the Medial Cerebellar Anlage of *Gbx2*-CKO Mutant Embryos Is Disrupted

To investigate the developmental basis of the cerebellar defect in *Gbx2*-CKO mice, we examined cerebellar formation at different developmental stages. In *Gbx2*-CKO embryos at E9.5, the isthmic constriction that normally

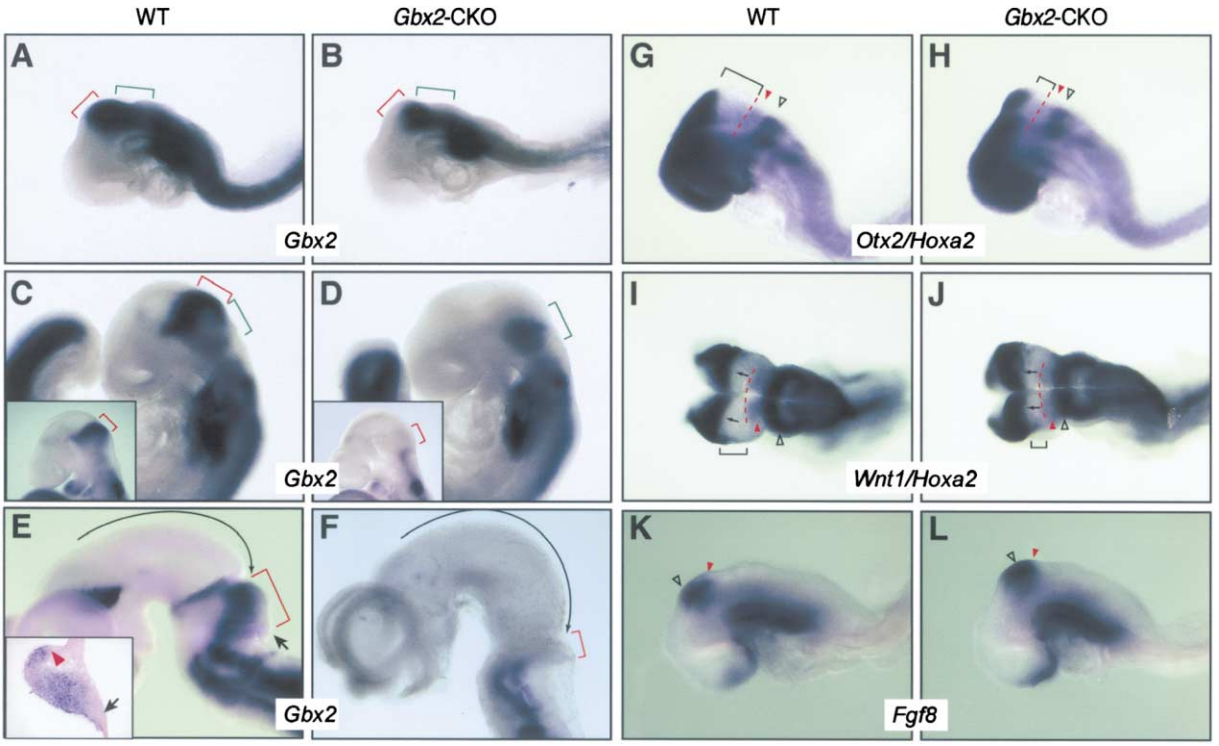

Figure 2. Progressive Loss of *Gbx2* in r1 of *Gbx2*-CKO Embryos from E8.5 to E9 and Posterior Shift of the mes/r1 Boundary into Anterior r1 at E8.5

(A–F) *Gbx2* expression in embryos of the genotypes indicated at the 8 somite stage (A and B), the 15 somite stage (C and D), and E9.5 (insets in [C] and [D]), and dissected E10.5 brains (E and F). Inset in (E) is a sagittal section through the cerebellar anlage showing that *Gbx2* is normally expressed broadly in the alar plate of r1, except in the prospective rhombic lips (arrow). The anterior expression domain of *Gbx2* in r1 is lost in *Gbx2*-CKO embryos at the 8 somite stage (compare [A] and [B]). In *Gbx2*-CKO embryos at the 15 somite stage and later, *Gbx2* expression in r1 (red brackets) is not detected, although *Gbx2* expression in r2-3 (green brackets) is still detected at the 15 somite stage (D). Note that the cerebellar anlage (marked by red brackets) is significantly reduced in size in *Gbx2*-CKO embryos at E10.5, whereas the mes (indicated by arrows) appears expanded posteriorly (compare [E] and [F]). (G–J) Double labeling for *Hoxa2* and *Otx2* (G and H) or *Hoxa2* and *Wnt1* (I and J) expression. The weak *Hoxa2* expression in r2 and the strong *Hoxa2* expression in r3 are marked by red and empty arrowheads, respectively. Red dashed lines demarcate the anterior limit of the *Hoxa2* expression domain in r2. Note that *Hoxa2* expression is not altered in the *Gbx2*-CKO embryos, but the size of r1 (brackets) is significantly reduced in the *Gbx2*-CKO embryos, as indicated by the cells negative for both *Hoxa2* and *Wnt1* or *Otx2*. The caudal border (black arrows) of *Wnt1* expression is sharp in wild-type embryos, whereas in *Gbx2*-CKO embryo the border is diffuse. (K and L) The center (empty arrowheads) of the *Fgf8* expression domain is shifted toward the border of r1/2 (red arrows) in *Gbx2*-CKO embryos. (A)–(H), (K), and (L) are lateral views of embryos, and (I) and (J) are dorsal views. Anterior is to the left.

divides the mes and r1 in the dorsal midline of the neural tube was less prominent (Figures 2D and 2F and see Figures 5 and 6). At E10.5, the mes expanded caudally, and the alar plate of r1 was significantly reduced in size (Figure 2F). Therefore, deletion of *Gbx2* specifically in r1 by E9 alters the morphology of the mes/r1 junction as early as E9.5, possibly leading to a posterior shift in its position and a reduction in the size of the cerebellar primordium by E10.5.

The cerebellum is a unique CNS structure that forms from two bilateral primordia that fuse in the dorsal midline. The vermis is thought to arise from the medial region where the fusion occurs. Consistent with the abnormal vermis seen in adult *Gbx2*-CKO mice, the medial region of the cerebellar primordium was reduced in size from E12.5 to E18.5 (Figure 4). To investigate whether this reduction was due to a decrease in cell proliferation, we analyzed brain sections by anti-BrdU immunohistochemistry after a 1 hr exposure to BrdU. In wild-type embryos at E12.5, the ventricular neuroepithelium of the cerebellar anlage contained a large number of BrdU-positive cells, with a higher accumulation of BrdU-positive cells in the medial region of the cerebellar anlage (Figure 4A). The neuroepithelium of the medial cerebellar anlage of E12.5 *Gbx2*-CKO mutants was thinner than normal, and abnormal indents were found in the ventricular layer (Figure 4B). Strikingly, the population of BrdU-positive cells seen in the medial region of wild-type cerebella was depleted in *Gbx2*-CKO mutants, although the proliferation in more lateral regions was not reduced (Figure 4B). In E14.5 *Gbx2*-CKO embryos, a local increase in the number of BrdU-positive cells was found in the indents and small cell aggregates in the cerebellar ventricular layer (Figure 4D). Likely related to high proliferation in the abnormal cell aggregates observed in the E14.5 cerebellar anlage, large cell aggregates were detected in cerebella of E18.5 *Gbx2*-CKO embryos (n = 6/6), mostly in the medial region (Figure 4F). Surprisingly, no cell aggregates were detected in 8 week or older *Gbx2*-CKO mutant cerebella (n = 0/6). These results show that the medial region of the cerebellar anlage is specifically reduced in size by E12.5 in *Gbx2*-CKO embryos, likely due to a reduction of cell proliferation in this region. In addition, abnormal cell aggregates form

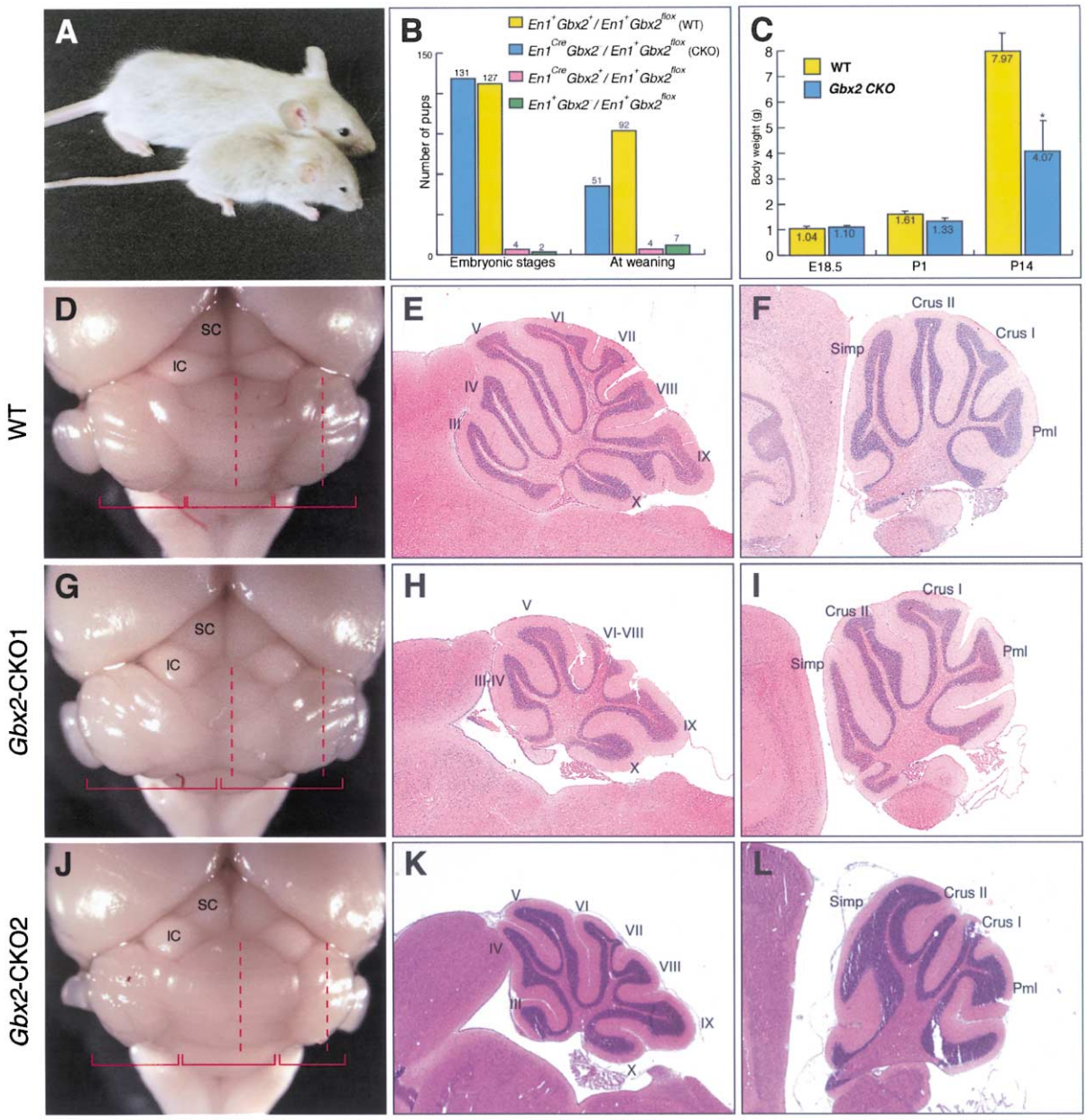

Figure 3. *Gbx2*-CKO Mutant Mice Are Runted and Develop a Cerebellum

(A) At 3 weeks of age, *Gbx2*-CKO mice (bottom) are significantly smaller than their normal littermates (top). (B) The number of embryos or pups at weaning of each genotype from crosses between $Gbx2^{flox/flox}$ and $En1^{Cre}$ $Gbx2^{-}/En1^{+}$ $Gbx2^{+}$ mice. The ratio between $En1^{Cre}$ $Gbx2^{-}/En1^{+}$ $Gbx2^{flox}$ to $En1^{+}$ $Gbx2^{+}/En1^{+}$ $Gbx2^{flox}$ decreases from approximately 100% (131/127) at embryonic stages to 55% (51/92) at weaning, suggesting that about 45% of *Gbx2*-CKO pups die before weaning. About 2.3% of $En1^{Cre}$ $Gbx2^{+}/En1^{+}$ $Gbx2^{flox}$ and $En1^{+}$ $Gbx2^{-}/En1^{+}$ $Gbx2^{flox}$ offspring result from recombination between the $En1^{Cre}$ and $Gbx2^{-}$ alleles in the parental male. (C) Histogram showing that *Gbx2*-CKO mutants have lower body weight than wild-type mice from postnatal day 1 (P1) and P14. (D, G, and J) Dorsal view of dissected posterior brain from adult wild-type (D) and *Gbx2*-CKO mutants with severe (G) and mild (J) phenotypes. (E, F, H, I, K, and L) Hematoxylin and eyosin (H&E) stained sagittal sections of the vermis (E, H, and K) and hemisphere (F, I, and L) of the cerebella shown in (D), (G), and (J). Sectioning plane is shown with dash lines. IC, inferior colliculus; Pml, paramedial lobe; SC, superior colliculus; Simp, simplex.

near the cerebellar ventricular layer in the medial region by E14.5 but are lost by 8 weeks of age.

Differential Ectopic Expression of *Otx2* and *Wnt1* in r1 of *Gbx2*-CKO Embryos

In order to understand the molecular mechanisms underlying the *Gbx2*-CKO mutant phenotype, we next analyzed the expression pattern of genes that are normally expressed in the mes/r1 junction region. As it has been shown that *Gbx2* negatively regulates *Otx2* and *Wnt1* expression (Li and Joyner, 2001; Liu and Joyner, 2001; Martinez-Barbera et al., 2001; Millet et al., 1999), we initially studied whether expression of *Otx2* or *Wnt1* was altered in *Gbx2*-CKO embryos. We compared the caudal limits of the expression domains of *Otx2* or *Wnt1* relative to the border between r1 and r2 by performing double

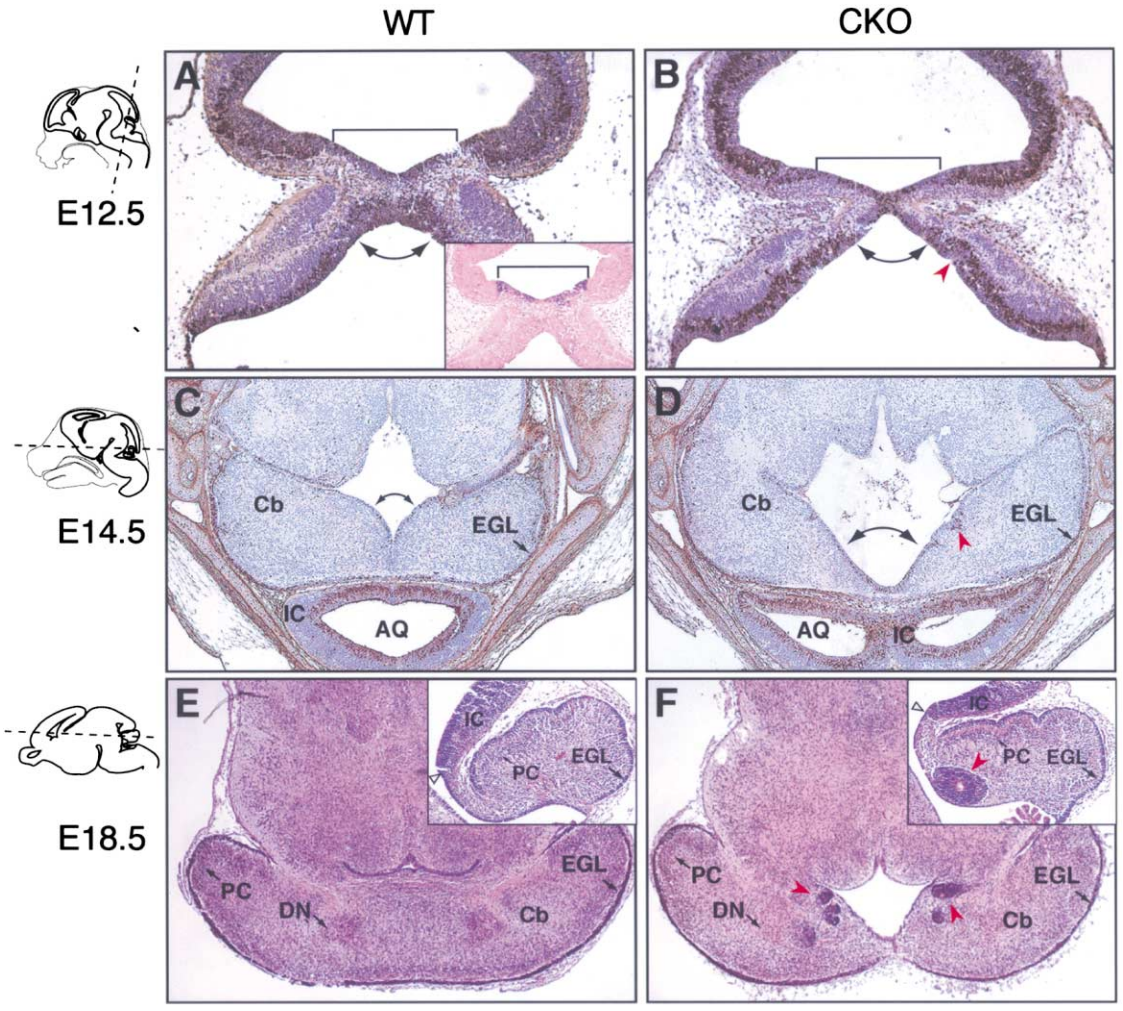

Figure 4. Abnormal Development of the Medial Cerebellar Anlage in *Gbx2*-CKO Embryos

(A–D) BrdU immunohistochemistry on coronal sections of developing cerebellum from E12.5 embryos (A and B) and on horizontal sections of the cerebellum from E14.5 embryos (C and D). Double curved arrows indicate the medial cerebellar anlage. Inset in (A) is *Fgf8* expression. Note the reduction in cell proliferation in the *Fgf8*-expressing domain (bracket). Abnormal indents and cell aggregates are marked by arrowheads. BrdU-positive and -negative cells are labeled as brown and blue, respectively.

(E and F) H&E stained horizontal sections of E18.5 cerebella. The prospective vermis in the cerebellum of the *Gbx2*-CKO mutant is greatly reduced in size, but the external granule layer (EGL), the deep nuclei (DN), and Purkinje cells (PC) appear to develop normally. Insets are medial sagittal sections of E18.5 cerebella showing the abnormal cell aggregates in *Gbx2*-CKO mutants. The mid/hindbrain junction is marked by empty arrowheads. Sectioning planes are shown as dash lines in the schematics. Rostral is to the top. AQ, aqueduct; Cb, cerebellum; IC, the inferior colliculus; PN, pons.

labeling for expression of *Hoxa2* and *Otx2* or of *Hoxa2* and *Wnt1*. At the 8 somite stage, *Hoxa2* is normally expressed strongly in r3 and r5 and weakly expressed in r2 (Figures 2G and 2I). In *Gbx2*-CKO mutants, *Hoxa2* expression appeared normal at the 8 somite stage and E9.5 (Figures 2H and 2J and data not shown). Significantly, at the 8 somite stage, the expression domains of *Otx2* and *Wnt1* were expanded caudally, and the distance between the posterior limit of the *Otx2* and *Wnt1* expression domains and *Hoxa2* expression in r2 was reduced in *Gbx2*-CKO embryos (Figures 2H and 2J). Interestingly, the expression domains of *Otx2* and *Wnt1* were apparently complementary to the remaining *Gbx2* expression in r1 at this stage (Figure 2B). Therefore, in *Gbx2*-CKO embryos, the expression domains of *Otx2* and *Wnt1* expand slightly posterior into r1 at the 8 somite stage.

Surprisingly, at E9.5, when *Gbx2* expression was no longer detected in r1 of *Gbx2*-CKO embryos, the *Otx2* expression domain was expanded only slightly posterior to the isthmic constriction around the dorsal midline of r1, forming a V shape with a diffuse caudal limit (Figure 5B). Furthermore, at E10.5, ectopic *Otx2* expression in r1 was mainly restricted to the dorsal midline and to a few scattered patches of cells weakly expressing *Otx2* in more posterior regions (Figure 5I). In contrast to the limited misexpression of *Otx2* in *Gbx2*-CKO embryos, the normally narrow transverse stripe of *Wnt1* expression in the mes (Figure 5C) was expanded posteriorly into r1 by E9.5 (Figure 5D), in the region corresponding

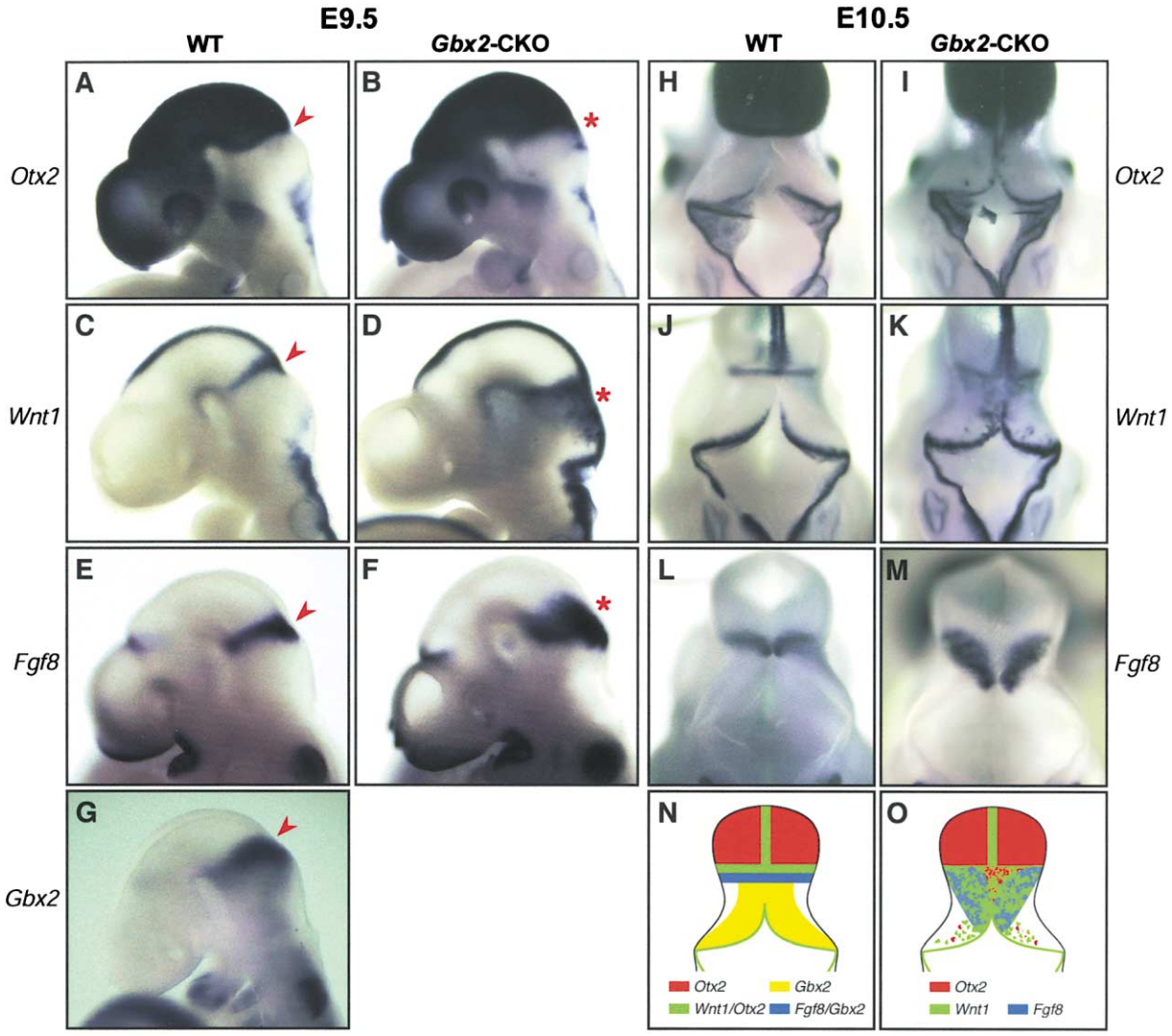

Figure 5. Differential Regulation of *Otx2*, *Wnt1*, and *Fgf8* in r1 of *Gbx2*-CKO Embryos at E9.5 and E10.5

(A–G) Lateral views of whole-mount E9.5 embryos labeled for expression of *Otx2* (A and B), *Wnt1* (C and D), *Fgf8* (E and F), and *Gbx2* (G). Note that the isthmic constriction (arrowheads and asterisks) is obscure in *Gbx2*-CKO mutants. The ectopic expression of *Wnt1* in r1 is found in the domain where *Gbx2* is normally expressed, and the ectopic expression of *Otx2* is less extensive compared to *Wnt1*.

(H–M) Dorsal views of whole-mount E10.5 embryos labeled for expression of *Otx2* (H and I), *Wnt1* (J and K), and *Fgf8* (L and M). The *Fgf8* expression domain is essentially complementary to the *Otx2* expression domain.

(N and O) Schematic representation of the expression of *Otx2*, *Wnt1*, *Gbx2*, and *Fgf8* in the mes/r1 region at E10.5.

to the domain where *Gbx2* is normally expressed (Figure 5G). At E10.5, scattered *Wnt1*-expressing cells were found throughout much of the alar plate of r1 (Figure 5K).

To compare the spatial distribution of the *Otx2* and *Wnt1* expression domains in more detail, we performed RNA in situ hybridization analysis on adjacent sagittal sections of E9.5 and E10.5 *Gbx2*-CKO embryos. Consistent with the whole-mount analysis in *Gbx2*-CKO embryos at E9.5, the *Wnt1* expression domain was expanded extensively into r1 beyond the posterior limit of the *Otx2* expression domain in both medial and lateral sections (Figures 6A–6F). At E10.5, *Wnt1* was still expressed extensively in r1, whereas only a few r1 cells, mostly in the dorsal midline, expressed *Otx2* (Figures 6J–6O). These results show that regulation of *Otx2* and *Wnt1* is differentially affected by the loss of *Gbx2* after E8.5, with *Wnt1* being ectopically expressed broadly in the r1 cells that normally express *Gbx2* at E9.5 and ectopic *Otx2* expression being restricted to the anterior and dorsal midline of r1. As a result, unlike the normal coexpression of *Wnt1* and *Otx2* in the mes, *Wnt1* is expressed in the absence of *Otx2* in many r1 cells of *Gbx2*-CKO mutants.

The *Fgf8* Expression Domain Partially Overlaps with *Wnt1* Expression and Opposes *Otx2* in *Gbx2*-CKO Embryos

To analyze whether loss of *Gbx2* after E9 alters formation of the mid/hindbrain organizer, we examined expression of *Fgf8* in *Gbx2*-CKO mutants. Consistent with the changes in *Otx2* and *Wnt1* expression at the 8 somite stage, the *Fgf8* expression domain was shifted slightly

posterior in *Gbx2*-CKO embryos (Figure 2L). Furthermore, at E9.5 and E10.5, the expression domain of *Fgf8* was both shifted and expanded posteriorly, particularly in the dorsal midline, such that the normally transverse band of *Fgf8*-expressing cells was transformed into a V shape, complementary to the expanded *Otx2* expression domain in r1 (Figures 5F and 5I versus 5M). Comparison of the expression domains of *Fgf8*, *Wnt1*, and *Otx2* on near adjacent sagittal sections of *Gbx2*-CKO embryos at E9.5 and E10.5 showed that the expression domain of *Fgf8* largely overlapped with that of *Wnt1* (Figure 6E versus 6H, 6F versus 6I). At E9.5, the expression domains of *Fgf8* and *Otx2* partially overlapped, and interestingly, in the region where *Otx2* and *Fgf8* overlapped, the expression levels of both genes appeared reduced (Figures 6B, 6C, 6H, and 6I). At E10.5, the expression domains of *Fgf8* and *Otx2* became complementary to each other, particularly in lateral regions (Figure 6K versus 6Q, 6L versus 6R). In summary, in *Gbx2*-CKO embryos, the *Fgf8* expression domain shifts posteriorly at the 8 somite stage relative to the new *Otx2*/*Gbx2* border in anterior r1. By E9.5 when *Gbx2* expression is completely abolished in r1, the *Fgf8* expression domain was expanded posteriorly, largely overlapping with *Wnt1* expression and becoming complementary to *Otx2* by E10.5.

Fgf8 Expression in the Isthmus Is Associated with Reduced Cell Proliferation

To investigate whether the ectopic expression of *Otx2*, *Wnt1*, and *Fgf8* in r1 persists in the developing cerebellum of *Gbx2*-CKO embryos, we analyzed expression of these genes after E10.5. In *Gbx2*-CKO embryos, few *Otx2*-expressing cells were detected in the alar plate of r1 in whole-mount E11.5 brains, and a few patches of weak *Otx2*-expressing cells were detected in sections of the E12.5 cerebellar anlage (Figure 7B). Of significance, the ectopic *Otx2*-expressing cells near the ventricular layer colocalized with the abnormal indents observed in this region (Figure 7B). In *Gbx2*-CKO embryos at E11.5 and E12.5, *Wnt1* expression was restricted to patches of cells in r1 (Figure 7D), in contrast to the more homogenous expression of *Wnt1* in the alar plate of r1 at E9.5 and E10.5 (Figures 5D and 5K). The patches of *Otx2* and *Wnt1* expressing cells did not appear to colocalize, similar to what was seen at earlier stages. Therefore, *Otx2* expression in r1 of *Gbx2*-CKO embryos was greatly reduced at E11.5 and E12.5, and ectopic *Wnt1* expression was not maintained in most r1 cells after E10.5.

Fgf8 is normally restricted to a transverse ring corresponding to the isthmic constriction at E11.5 and E12.5 (Figure 7E). The *Fgf8* expression domain was expanded posteriorly in what appeared to be an enlarged isthmus in *Gbx2*-CKO mutants at E11.5 and E12.5 (Figure 7F). Interestingly, we found that the level of cell proliferation in the region of *Fgf8* expression was remarkably lower than in adjacent cells in both wild-type and *Gbx2*-CKO embryos (Figures 4A and 4B). This raises the question of whether the expanded *Fgf8* expression domain at E11.5 and E12.5 contributes to the reduction in cell proliferation and thus in the size of the medial cerebellar anlage of *Gbx2*-CKO embryos.

Cell Aggregates in the Cerebellum of *Gbx2*-CKO Embryos Express *Otx2* and Have Molecular Characteristics of the Inferior Colliculus

In *Gbx2*-CKO embryos at E14.5, the expression of *Wnt1* and *Fgf8* in the isthmus was greatly reduced as in wild-type embryos, and no ectopic expression of *Wnt1* and *Fgf8* was detected in the cerebellum (data not shown). In contrast, strong *Otx2* expression was found at E14.5 in the abnormal cell aggregates seen near the ventricular layer of the cerebellum (Figure 7H). In addition, the number of *Otx2*-expressing cells seems to increase after E12.5, which may be related to the finding that at E14.5 the ectopic *Otx2*-expressing cells were highly proliferative based on BrdU labeling (data not shown). To investigate whether the increased expression of *Otx2* transforms cells in the abnormal aggregates into a midbrain fate, we examined expression of *EphrinA5*, which is normally expressed in the inferior colliculus (Donoghue et al., 1996) (Figure 7I). Significantly, *EphrinA5* was not detected in r1 at E12.5 (data not shown) but became ectopically expressed in the cell aggregates at E14.5 (Figure 7J). Therefore, ectopic expression of *Otx2* but not *Wnt1* and *Fgf8* persists in the developing cerebellum of *Gbx2*-CKO embryos. Furthermore, the *Otx2*-expressing cells coexpress *EphrinA5* and become segregated from neighboring cells forming large ectopic structures within the cerebellum by E14.5.

Discussion

A *Gbx2*-Independent Mechanism Can Repress *Otx2* in r1 after E8.5

Although an essential role for *Gbx2* in repression of *Otx2* prior to the early somite stages had been demonstrated (Li and Joyner, 2001; Martinez-Barbera et al., 2001), it was unclear whether *Gbx2* continues to be required to repress *Otx2* in r1 at later stages. Analysis of the changes in *Otx2* expression in response to a loss of *Gbx2* in r1 from the 8 to 15 somite stage in *Gbx2*-CKO embryos allowed us to dissect the temporal requirement for *Gbx2* in repression of *Otx2*. The expression domains of *Gbx2* and *Otx2* were normal in *Gbx2*-CKO embryos at the 6 somite stage (data not shown). By the 8 somite stage, however, the *Otx2* expression domain was already expanded posteriorly into the r1 cells that had lost *Gbx2* expression. This rapid change in *Otx2* expression shows that repression of *Otx2* in r1 is highly dependent on *Gbx2* function at the 6 to 8 somite stages. To our surprise, deletion of *Gbx2* in the rest of r1 by the 15 somite stage did not result in ectopic expression of *Otx2* throughout the alar plate of r1 where *Gbx2* is normally expressed. Instead, we found that ectopic *Otx2* expression was largely restricted to a small dorsal and medial domain of anterior r1. These results demonstrate that after the 8 somite stage a *Gbx2*-independent pathway is involved in repressing *Otx2* in posterior r1.

It is possible that an unknown factor is induced in r1 after the 8 somite stage that can replace the function of Gbx2 in repressing *Otx2* in r1. Another possibility is that *Otx2* expression in r1 of *Gbx2*-CKO embryos is repressed by Fgf8, which is induced in r1 at the 3 to 5 somite stage. Consistent with this, we previously showed that Fgf8-soaked beads can repress *Otx2* ex-

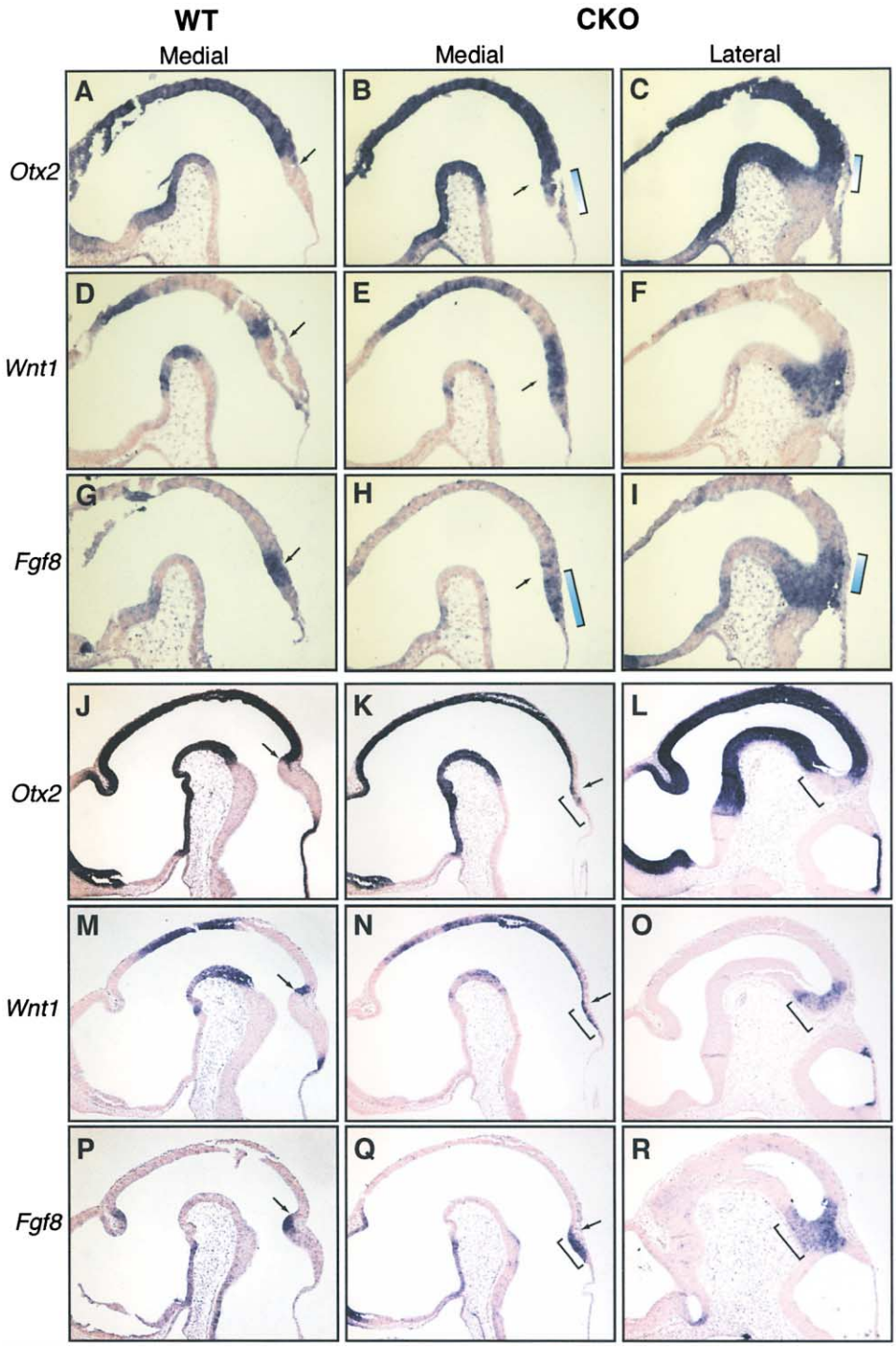

Figure 6. The *Fgf8* Expression Domain Partially Overlaps with *Wnt1* and Opposes *Otx2* in *Gbx2*-CKO Embryos

(A–I) RNA in situ hybridization of *Otx2* (A–C), *Wnt1* (D–F), and *Fgf8* (G–I) on sagittal sections of wild-type and *Gbx2*-CKO embryos at E9.5. The left column represents medial sections of wild-type embryos, the middle and right columns represent medial and lateral sections, respectively, of *Gbx2*-CKO embryos. The anterior border of r1 is defined as the middle of the constriction (arrows). Note that in *Gbx2*-CKO embryos the expression domain of *Fgf8* in r1 largely encompasses *Wnt1* expression and partially overlaps with *Otx2* at E9.5. In the region where the expression domains of *Otx2* and *Fgf8* overlap (brackets), *Fgf8* and *Otx2* are expressed as opposing gradients, as indicated by the shading in the bracket.

(J–R) Expression of *Otx2* (J–L), *Wnt1* (M–O), and *Fgf8* (P–R) in midline sections of wild-type and midline and lateral sections of *Gbx2*-CKO embryos at E10.5. Note that *Wnt1* is still expressed broadly in r1, largely colocalized with *Fgf8* expression, and that the expression domain of *Otx2* is complementary to that of *Fgf8*, particularly in lateral regions.

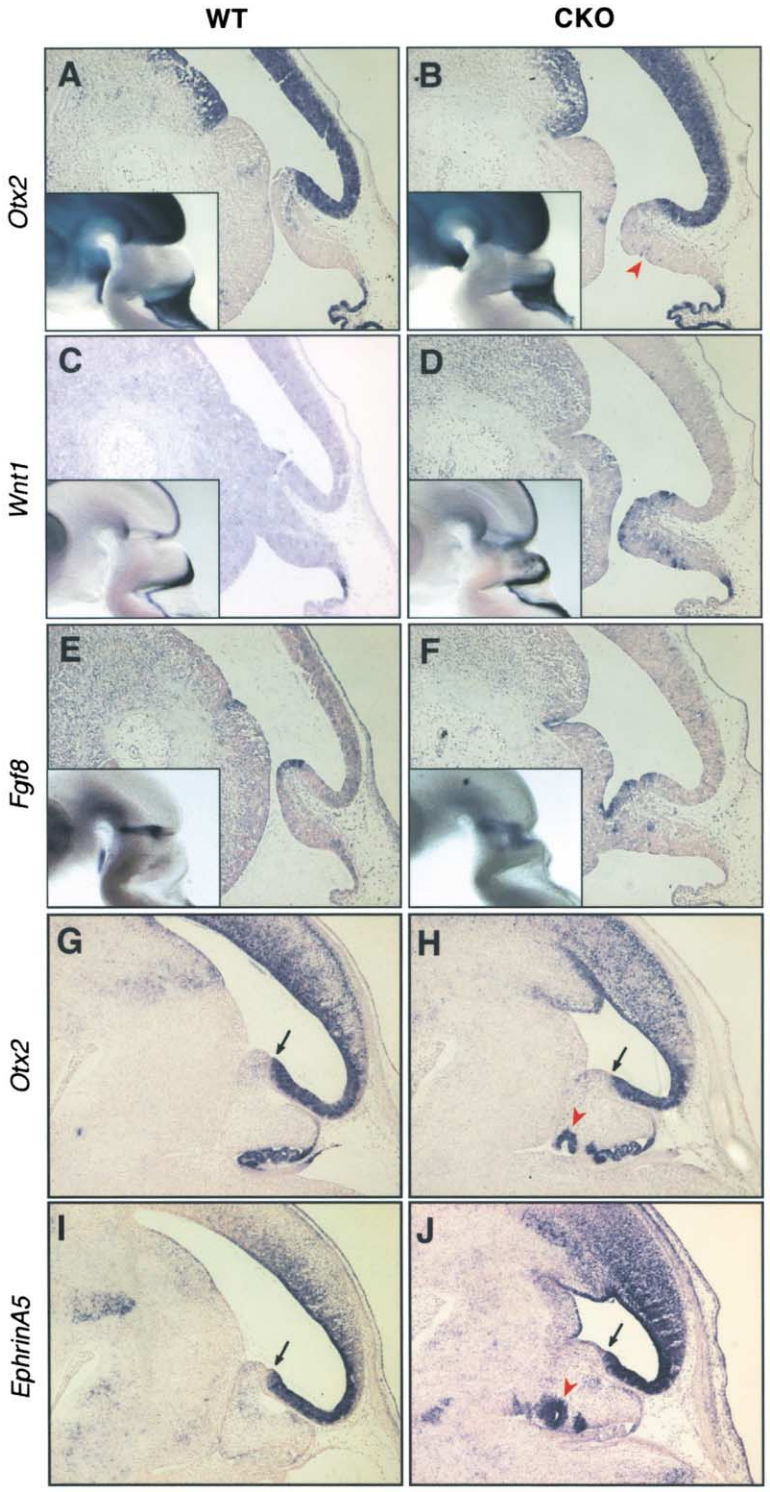

Figure 7. Increased Expression of *Otx2* in the Cerebellar Anlage of *Gbx2*-CKO Embryos after E12.5

(A–F) Expression of *Otx2* (A and B), *Wnt1* (C and D), and *Fgf8* (E and F) in sagittal brain sections of E12.5 wild-type and *Gbx2*-CKO embryos. Insets in (A)–(F) show expression of *Otx2*, *Wnt1*, and *Fgf8* in E11.5 whole-mount brains. Ectopic expression of *Otx2* in the cerebellum of the *Gbx2*-CKO embryos is weak compared to expression in the midbrain, and abnormal indents in the ventricular layer are associated with the presence of patches of *Otx2*-expressing cells (arrowhead).

(G–J) Expression of *Otx2* (G and H) and *EphrinA5* (I and J) in adjacent sagittal sections of wild-type or *Gbx2*-CKO embryos at E14.5. Note that, in contrast to the weak and scattered *Otx2* expression in the cerebellum of *Gbx2*-CKO embryos at E12.5, ectopic *Otx2* is strong and confined to the abnormal cell aggregates (arrowheads) near the ventricular zone at E14.5, colocalizing with *EphrinA5* expression. Arrows mark the mid/hindbrain junction. Ventral is to the left, and anterior is to the top.

pression in diencephalic explants independent of *Gbx2* (Liu and Joyner, 2001). Several additional observations support the proposal that after E9.5 in *Gbx2*-CKO mutants Fgf8 determines the posterior limit of *Otx2* expression in r1. By E9.5 in *Gbx2*-CKO mutants, *Fgf8* expression was expanded posteriorly, encompassing the posterior alar plate of r1 in a domain complementary to *Otx2* expression. Although the anterior expression domain of *Fgf8* overlapped with the posterior expression domain of *Otx2* at E9.5, the expression levels of *Otx2* and *Fgf8* appeared reduced in the region of overlap, consistent with the proposed mutual negative regulation between *Otx2* and *Fgf8* (Liu and Joyner, 2001; Liu et al., 1999; Martinez et al., 1999). Furthermore, the expression domains of *Otx2* and *Fgf8* became largely complementary with each other by E10.5, and only a few patches

of weak *Otx2*-expressing cells were found in r1 at E10.5 and E12.5. Therefore, our results are consistent with Fgf8 compensating for the loss of *Gbx2* function in repressing *Otx2* after the 15 somite stage.

Our suggestion that *Fgf8* negatively regulates *Otx2* in *Gbx2*-CKO embryos after E9.5 could be considered contradictory to our previous findings that in *Gbx2* null mutant embryos or in embryos lacking both *Gbx2* and *Otx2* function the expression domains of *Fgf8* and *Otx2* overlap at E9.5 and E10.5. One possible explanation for this could relate to the fact that *Fgf8* undergoes differential splicing that produces various isoforms, including Fgf8a and Fgf8b (Crossley and Martin, 1995; MacArthur et al., 1995). Experiments in chick and mouse embryos have shown that Fgf8b but not Fgf8a can effectively repress *Otx2* (Sato et al., 2001). One possibility is that Fgf8a is dominantly expressed in *Gbx2* or in *Gbx2* and *Otx2* double mutant embryos, whereas Fgf8b is responsible for repressing *Otx2* in r1 of normal and *Gbx2*-CKO mutants.

Gbx2 Is Required to Maintain a Normal Mid/Hindbrain Organizer

In *Gbx2*-CKO embryos, the juxtaposition of the *Wnt1* and *Fgf8* expression domains was present at the 8 somite stage, but, consistent with previous studies showing that an interaction between *Otx2* and *Gbx2* positions the mid/hindbrain organizer (Broccoli et al., 1999; Katahira et al., 2000; Millet et al., 1999), the border was shifted posteriorly to the new *Otx2*/*Gbx2* border. In contrast, at E9.5 when *Gbx2* transcripts were no longer detected in r1, *Wnt1* and *Fgf8* were broadly coexpressed in the alar plate of r1. The derepression of *Wnt1* in the alar plate of r1 where *Gbx2* is normally expressed demonstrates a cell-autonomous requirement for Gbx2 in repression of *Wnt1* expression after E9.5, in agreement with previous studies (Liu and Joyner, 2001; Li and Joyner, 2001; Martinez-Barbera et al., 2001). As it has been reported that ectopic expression of *Wnt1* in r1 can induce *Fgf8* in chick embryos (Ye et al., 2001), derepression of *Wnt1* in r1 cells in *Gbx2*-CKO embryos could contribute to the expansion of *Fgf8* expression in this region. Furthermore, we found that the expression domain of *Pax2* in the isthmus was expanded posteriorly in *Gbx2*-CKO embryos from E9.5 and largely overlapped with that of *Fgf8* (data not shown), consistent with a previous study showing that Pax2 is essential for induction of *Fgf8* (Ye et al., 2001). Taken together with previous studies, our current experiments show that *Gbx2* is required from E8.5 onward to repress *Wnt1* expression in r1 and maintain the normal relative expression domains of *Wnt1* and *Fgf8*.

Gbx2 Is Not Essential for Cerebellar Development after E9

Analysis of null mutants previously demonstrated that *Gbx2* is essential for development of r1-3, including the cerebellum (Wassarman et al., 1997). Furthermore, it was shown that loss of r1-3 in *Gbx2* null mutants could be due to the rapid posterior expansion of *Otx2* into this region at E7.75 (Li and Joyner, 2001; Martinez-Barbera et al., 2001; Millet et al., 1999). Consistent with this, we have shown that removal of *Otx2* rescues r3 development in *Gbx2* homozygous mutant embryos, demonstrating that *Gbx2* promotes development in r3 mainly by repressing *Otx2* (Li and Joyner, 2001). However, the specific role of *Gbx2* in cerebellar development after its initial requirement to repress *Otx2* in r1 was not clear. In this study, we show that the cerebellum can develop with remarkably normal cerebellar hemispheres in mouse embryos deficient in *Gbx2* after E9, although formation of the vermis is partially repressed. Furthermore, no cytological defects were detected in the vermis or hemispheres of *Gbx2*-CKO cerebella. Collectively, our data demonstrate the differential temporal requirements for *Gbx2* in cerebellar development. Between E7.75 and E9, *Gbx2* is crucial for specification of the cerebellar primordium by repressing *Otx2* expression, and thereafter, *Gbx2* is not essential for development of the cerebellum. Furthermore, our studies raise the question of whether Gbx2 is actually required in Fgf8b misexpression studies in which cerebellar tissue is induced.

The Reduction in Vermis Development in *Gbx2*-CKO Mutants Could Be Caused by Ectopic Expression of *Otx2* and/or *Fgf8*

Removal of *Gbx2* in r1 after E9 was found to specifically inhibit development of medial cerebellar structures. Of interest, a similar vermis-specific cerebellar defect is found in mice that express *Otx2* in r1 from the *En1* locus (*En1*$^{+/Otx2}$), although the defect is accompanied by a significant expansion of the midbrain (Broccoli et al., 1999). Similar to *Gbx2*-CKO mutants, the caudal limit of *Otx2* expression is shifted into the anterior and dorsal midline of r1 in *En1*$^{+/Otx2}$ mutants at E9.5. However, unlike in *Gbx2*-CKO mutants, *Gbx2* is still expressed in r1 cells posterior to the ectopic *Otx2* expression domain in *En1*$^{+/Otx2}$ embryos. The similarity of the cerebellar phenotypes in the two mutants and our finding that *Gbx2* is not required for development of the remaining cerebellum could be taken to suggest that the ectopic expression of *Otx2* is involved in inhibiting vermis development in both mutants. In support of this, the cerebellar phenotype in *En1*$^{+/Otx2}$ mutants appears to be more severe than in *Gbx2*-CKO mutants, and the ectopic expression domain of *Otx2* is more extensive in *En1*$^{+/Otx2}$ embryos than in *Gbx2*-CKO mutants at E12.5 (Broccoli et al., 1999).

A number of findings in our *Gbx2*-CKO mutants suggest that the misexpression of *Otx2* alone may not account for the cerebellar defect in these mutants. First, *Otx2* is expressed only weakly in a few r1 cells at E11.5 and E12.5 in *Gbx2*-CKO mutants, despite the medial cerebellar anlage being significantly reduced in size at E12.5. Furthermore, in *Gbx2*-CKO embryos at E11.5 and E12.5, the *Fgf8* expression domain is abnormally expanded and resides in the affected region, correlating with an area of reduced cell proliferation. Similarly, using BrdU labeling at E12.5, we found that *Fgf8* is normally expressed in the isthmus and that cells in the isthmus undergo lower proliferation than in adjacent regions. The latter finding is in agreement with a previous study showing a reduction of cell proliferation in the isthmus using ^{3}H-thymidine labeling (Altman and Bayer, 1997).

Taken together, the studies suggest that Fgf8 could normally reduce cell proliferation in the isthmus, and in

Gbx2-CKO mutants, it also decreases proliferation in the medial cerebellar anlage. In agreement with Fgf8 having the potential to suppress cell proliferation, it was recently found that Fgf8-soaked beads placed in the forebrain can lead to a reduction in proliferation of nearby cells (Crossley et al., 2001). Furthermore, ectopic expression of Fgf8b in the chick mes causes a significant reduction in the size of the midbrain vesicle, in contrast to a mitogenic effect of Fgf8a on the midbrain (Sato et al., 2001). In summary, we propose that in *Gbx2*-CKO mutants, ectopic expression of Fgf8b in the medial cerebellar anlage leads to a decrease in cell proliferation and, consequently, a reduction in the vermis anlage. At the same time, Fgf8b represses *Otx2* in r1, allowing development of the lateral cerebellum.

How Transcription Factor Functions Can Change during Development

Development of the CNS involves highly combinatorial actions of transcription factors. Previous studies and our current analysis demonstrate that a given transcription factor can have multiple functions during development, both within the same tissue and in different organs. One common mechanism to achieve multiple roles for a transcription factor is through a sequential change in binding partners. Indeed, during vertebrate CNS development, an interaction between the *Drosophila* Groucho homolog Grg4 and Pax 2/5 proteins changes the Pax proteins from being transcriptional activators to repressors (Sugiyama, et al., 2000; Ye et al., 2001). Similarly, during *Drosophila* mesoderm development, the basic helix-loop-helix transcription factor Twist can promote or repress somatic muscle development depending on its dimerization partners (Castanon, et al., 2001). Interestingly, we demonstrated in this work that *Gbx2* is initially required to repress *Otx2* before E8.5 to allow specification of the cerebellar primordium. After E8.5, *Gbx2* is not essential for the repression of *Otx2* because a second pathway is induced that can repress *Otx2*. *Gbx2* is nevertheless still required for maintenance of normal expression of *Wnt1* and *Fgf8*. The temporal changing requirement for Gbx2 during cerebellar development demonstrated in this work provides a different paradigm for how the same transcription factor can control sequential events during a single developmental process.

Experimental Procedures

Homologous Recombination in ES Cells

One *loxP* site was inserted into a BamHI site in the intron, and another *loxP* site into an NcoI site in the 3′ untranslation region of *Gbx2* (see Figure 1A). Cre-mediated DNA recombination will delete most of the second exon of *Gbx2*, which encodes the homeodomain, generating an allele similar to the original *Gbx2* null allele (Wassarman et al., 1997). The selectable marker genes *neo* and *tk*, used for the gene targeting in ES cells, were placed immediately upstream of the 5′-*loxP* site and the 5′ homologous arm, respectively. The *neo* cassette was flanked by *Frt* sequences and thus could be removed by Flpe-mediated DNA recombination. Homologous recombination in W4 ES cells (Auerbach et al., 2000) was performed as described previously (Matise et al., 2000). Seventeen targeted ES cell clones ($Gbx2^{+/flox\text{-}neo}$) were identified from 136 G418 and GANC resistant cell clones by Southern blot analysis (see Figure 1B). ES cell chimeras were generated through injection of C57BL/6 blastocysts with three independently targeted ES cell clones (1A11, 1F8, and 1F9). Heterozygous $Gbx2^{+/flox\text{-}neo}$ mice were produced by breeding chimeric males with wild-type C57BL/6 females. $Gbx2^{+/flox\text{-}neo}$ mice were subsequently bred to *hACTB-Flpe* mice (Rodriguez et al., 2000), which express *Flpe* broadly under the control of a human β-*actin* promoter, to produce heterozygous mice with a *Gbx2* conditional mutant allele, $Gbx2^{+/flox}$. $Gbx2^{+/flox}$ mice derived from 1A11 and 1F9 ES cell clones produced the same phenotypes, and data were pooled from these two lines.

Mouse Breeding and Genotyping

Noon of the day on which the vaginal plug was detected was designated as E0.5 in timing of embryos. Embryos with 8 or 15 somites are designated as E8.5 and E9, respectively. Double heterozygous $En1^{Cre}\,Gbx2^{+}/En1^{+}\,Gbx2^{-}$ mice were generated by crossing $En1^{+/Cre}$ mice (Kimmel et al., 2000) with $Gbx2^{+/-}$ mice (Wassarman et al., 1997). The $En1^{Cre}\,Gbx2^{+}/En1^{+}\,Gbx2^{-}$ mice were then bred with Swiss Webster wild-type mice to produce double heterozygous mice ($En1^{Cre}\,Gbx2^{-}/En1^{+}\,Gbx2^{+}$) carrying both mutant alleles on the same chromosome. These double heterozygous mice were bred to $Gbx2^{flox/flox}$ mice to generate *Gbx2*-CKO mutants. Genotyping was carried out by PCR analysis (see Figures 1A and 1C). The primers used for PCR genotyping were a, 5′-CTGTTCACGTTAGCAGG TTCGC; b, 5′-TGCTTGGATGTCCACATCTAGG; Cre-f, 5′-TAAAGAT ATCTCACGTACTGACGGTG; Cre-r, 5′-TCTCTGACCAGAGTCATCC TTAGC.

BrdU Labeling

For Bromodeoxyuridine (BrdU) labeling experiments, pregnant females were injected intraperitoneally with 100 μg BrdU/g body weight 1 hr before they were sacrificed. Embryo processing and BrdU labeling were performed as described previously (Mishina et al., 1995).

RNA In Situ Hybridization and Histological Analysis

X-gal staining of whole-mount embryos was performed according to standard procedures (Hogan et al., 1994). RNA in situ hybridization analysis of whole-mount embryos or sections was performed as described (Li and Joyner, 2001). The antisense RNA probes were as described previously: *EphrinA5* (*RAGS*) (Flenniken et al., 1996), *Fgf8* (Crossley and Martin, 1995), *Hoxa2* (Wilkinson et al., 1989), *Otx2* (Ang et al., 1994), and *Wnt1* (Parr et al., 1993). A *Gbx2* probe corresponding to the exon sequences flanked by the *loxP* sites was generated by PCR using *Gbx2* cDNA as template and cloned into the *pCRII* vector (Invitrogen). The primers used for the PCR reaction were 5′-GGAAAGACGAGTCAAAGG-3′ and 5′-TGCTTGGATGTC CACATCTAGG-3′.

Acknowledgments

We thank Drs. G. Martin, A. McMahon, F. Rijli, and J. Rossant for providing probes for RNA in situ hybridization analysis. We are also grateful to Cindy Chen and Qiuxia Guo for technical help and to Dr. Mark Zervas and Sema Sgaier for critical reading of the manuscript. J.Y.H.L was a Howard Hughes Medical Institute (HHMI) research associate during the early stages of the study and is currently supported by a National Institutes of Health postdoctoral fellowship. A.L.J. is an HHMI investigator.

Received: June 7, 2002
Revised: August 5, 2002

References

Acampora, D., Mazan, S., Lallemand, Y., Avantaggiato, V., Maury, M., Simeone, A., and Brulet, P. (1995). Forebrain and midbrain regions are deleted in $Otx2^{-/-}$ mutants due to a defective anterior neuroectoderm specification during gastrulation. Development *121*, 3279–3290.

Altman, J., and Bayer, S.A. (1997). Development of the Cerbellar System: In Relation to Its Evolution, Structure, and Functions (New York: CRC Press).

Ang, S.L., Conlon, R.A., Jin, O., and Rossant, J. (1994). Positive and

negative signals from mesoderm regulate the expression of mouse Otx2 in ectoderm explants. Development *120*, 2979–2989.

Ang, S.L., Jin, O., Rhinn, M., Daigle, N., Stevenson, L., and Rossant, J. (1996). A targeted mouse Otx2 mutation leads to severe defects in gastrulation and formation of axial mesoderm and to deletion of rostral brain. Development *122*, 243–252.

Auerbach, W., Dunmore, J.H., Fairchild-Huntress, V., Fang, Q., Auerbach, A.B., Huszar, D., and Joyner, A.L. (2000). Establishment and chimera analysis of 129/SvEv- and C57BL/6-derived mouse embryonic stem cell lines. Biotechniques *29*, 1024–1028.

Bouillet, P., Chazaud, C., Oulad-Abdelghani, M., Dolle, P., and Chambon, P. (1995). Sequence and expression pattern of the Stra7 (Gbx-2) homeobox-containing gene induced by retinoic acid in P19 embryonal carcinoma cells. Dev. Dyn. *204*, 372–382.

Broccoli, V., Boncinelli, E., and Wurst, W. (1999). The caudal limit of Otx2 expression positions the isthmic organizer. Nature *401*, 164–168.

Castanon, I., Von Stetina, S., Kass, J., and Baylies, M.K. (2001). Dimerization partners determine the activity of the Twist bHLH protein during Drosophila mesoderm development. Development *128*, 3145–3159.

Chapman, G., Remiszewski, J.L., Webb, G.C., Schulz, T.C., Bottema, C.D., and Rathjen, P.D. (1997). The mouse homeobox gene, Gbx2: genomic organization and expression in pluripotent cells in vitro and in vivo. Genomics *46*, 223–233.

Crossley, P.H., and Martin, G.R. (1995). The mouse Fgf8 gene encodes a family of polypeptides and is expressed in regions that direct outgrowth and patterning in the developing embryo. Development *121*, 439–451.

Crossley, P.H., Martinez, S., and Martin, G.R. (1996). Midbrain development induced by FGF8 in the chick embryo. Nature *380*, 66–68.

Crossley, P.H., Martinez, S., Ohkubo, Y., and Rubenstein, J.L. (2001). Coordinate expression of Fgf8, Otx2, Bmp4, and Shh in the rostral prosencephalon during development of the telencephalic and optic vesicles. Neuroscience *108*, 183–206.

Donoghue, M.J., Lewis, R.M., Merlie, J.P., and Sanes, J.R. (1996). The Eph kinase ligand AL-1 is expressed by rostral muscles and inhibits outgrowth from caudal neurons. Mol. Cell. Neurosci. *8*, 185–198.

Flenniken, A.M., Gale, N.W., Yancopoulos, G.D., and Wilkinson, D.G. (1996). Distinct and overlapping expression patterns of ligands for Eph-related receptor tyrosine kinases during mouse embryogenesis. Dev. Biol. *179*, 382–401.

Garda, A.L., Echevarria, D., and Martinez, S. (2001). Neuroepithelial co-expression of Gbx2 and Otx2 precedes Fgf8 expression in the isthmic organizer. Mech. Dev. *101*, 111–118.

Hatten, M.E., and Heintz, N. (1995). Mechanisms of neural patterning and specification in the developing cerebellum. Annu. Rev. Neurosci. *18*, 385–408.

Hogan, B.M., Beddington, R., Costantini, F., and Lacy, E. (1994). Manipulating the Mouse Embryo: A Laboratory Manual (Cold Spring Harbor, NY: Cold Spring Harbor Press).

Joyner, A.L., Liu, A., and Millet, S. (2000). Otx2, Gbx2 and Fgf8 interact to position and maintain a mid-hindbrain organizer. Curr. Opin. Cell Biol. *12*, 736–741.

Katahira, T., Sato, T., Sugiyama, S., Okafuji, T., Araki, I., Funahashi, J., and Nakamura, H. (2000). Interaction between otx2 and gbx2 defines the organizing center for the optic tectum. Mech. Dev. *91*, 43–52.

Kimmel, R.A., Turnbull, D.H., Blanquet, V., Wurst, W., Loomis, C.A., and Joyner, A.L. (2000). Two lineage boundaries coordinate vertebrate apical ectodermal ridge formation. Genes Dev. *14*, 1377–1389.

Li, J.Y., and Joyner, A.L. (2001). Otx2 and Gbx2 are required for refinement and not induction of mid-hindbrain gene expression. Development *128*, 4979–4991.

Liu, A., and Joyner, A.L. (2001). Early anterior/posterior patterning of the midbrain and cerebellum. Annu. Rev. Neurosci. *24*, 869–896.

Liu, A., Losos, K., and Joyner, A.L. (1999). FGF8 can activate Gbx2 and transform regions of the rostral mouse brain into a hindbrain fate. Development *126*, 4827–4838.

MacArthur, C.A., Lawshe, A., Xu, J., Santos-Ocampo, S., Heikinheimo, M., Chellaiah, A.T., and Ornitz, D.M. (1995). FGF-8 isoforms activate receptor splice forms that are expressed in mesenchymal regions of mouse development. Development *121*, 3603–3613.

Martinez, S., Crossley, P.H., Cobos, I., Rubenstein, J.L., and Martin, G.R. (1999). FGF8 induces formation of an ectopic isthmic organizer and isthmocerebellar development via a repressive effect on Otx2 expression. Development *126*, 1189–1200.

Martinez-Barbera, J.P., Signore, M., Boyl, P.P., Puelles, E., Acampora, D., Gogoi, R., Schubert, F., Lumsden, A., and Simeone, A. (2001). Regionalisation of anterior neuroectoderm and its competence in responding to forebrain and midbrain inducing activities depend on mutual antagonism between OTX2 and GBX2. Development *128*, 4789–4800.

Matise, M.P., Auerbach, W., and Joyner, A.L. (2000). Production of targeted embryonic stem cell clones. In Gene Targeting, A.L. Joyner, ed. (New York, Oxford University Press), pp. 101–132.

Matsuo, I., Kuratani, S., Kimura, C., Takeda, N., and Aizawa, S. (1995). Mouse Otx2 functions in the formation and patterning of rostral head. Genes Dev. *9*, 2646–2658.

Millen, K.J., Wurst, W., Herrup, K., and Joyner, A.L. (1994). Abnormal embryonic cerebellar development and patterning of postnatal foliation in two mouse Engrailed-2 mutants. Development *120*, 695–706.

Millet, S., Campbell, K., Epstein, D.J., Losos, K., Harris, E., and Joyner, A.L. (1999). A role for Gbx2 in repression of Otx2 and positioning the mid/hindbrain organizer. Nature *401*, 161–164.

Mishina, Y., Suzuki, A., Ueno, N., and Behringer, R.R. (1995). Bmpr encodes a type I bone morphogenetic protein receptor that is essential for gastrulation during mouse embryogenesis. Genes Dev. *9*, 3027–3037.

Parr, B.A., Shea, M.J., Vassileva, G., and McMahon, A.P. (1993). Mouse Wnt genes exhibit discrete domains of expression in the early embryonic CNS and limb buds. Development *119*, 247–261.

Rodriguez, C.I., Buchholz, F., Galloway, J., Sequerra, R., Kasper, J., Ayala, R., Stewart, A.F., and Dymecki, S.M. (2000). High-efficiency deleter mice show that FLPe is an alternative to Cre-loxP. Nat. Genet. *25*, 139–140.

Sato, T., Araki, I., and Nakamura, H. (2001). Inductive signal and tissue responsiveness defining the tectum and the cerebellum. Development *128*, 2461–2469.

Shamim, H., Mahmood, R., Logan, C., Doherty, P., Lumsden, A., and Mason, I. (1999). Sequential roles for Fgf4, En1 and Fgf8 in specification and regionalisation of the midbrain. Development *126*, 945–959.

Soriano, P. (1999). Generalized lacZ expression with the ROSA26 Cre reporter strain. Nat. Genet. *21*, 70–71.

Sugiyama, S., Fuahashi, J., and Nakamura, H. (2000). Antagonizing activity of chick Grg4 against tectum-organizing activity. Dev. Biol. *221*, 168–180.

Wassarman, K.M., Lewandoski, M., Campbell, K., Joyner, A.L., Rubenstein, J.L., Martinez, S., and Martin, G.R. (1997). Specification of the anterior hindbrain and establishment of a normal mid/hindbrain organizer is dependent on Gbx2 gene function. Development *124*, 2923–2934.

Wilkinson, D.G., Bhatt, S., Cook, M., Boncinelli, E., and Krumlauf, R. (1989). Segmental expression of Hox-2 homoeobox-containing genes in the developing mouse hindbrain. Nature *341*, 405–409.

Wingate, R.J. (2001). The rhombic lip and early cerebellar development. Curr. Opin. Neurobiol. *11*, 82–88.

Ye, W., Bouchard, M., Stone, D., Liu, X., Vella, F., Lee, J., Nakamura, H., Ang, S.L., Busslinger, M., and Rosenthal, A. (2001). Distinct regulators control the expression of the mid-hindbrain organizer signal FGF8. Nat. Neurosci. *4*, 1175–1181.